Pergamon
www.elsevier.nl/locate/asr

Adv. Space Res. Vol. 25, No. 1, pp. 163–169, 2000

Printed in Great Britain
0273-1177/00 $20.00 + 0.00
PII: S0273-1177(99)00914-X

GLOBAL EMPIRICAL MODEL OF ELECTRON TEMPERATURE IN THE OUTER IONOSPHERE FOR PERIOD OF HIGH SOLAR ACTIVITY BASED ON DATA OF THREE INTERCOSMOS SATELLITES

V. Truhlík[1], L. Třísková[1], J. Šmilauer[1], and V.V. Afonin[2]

[1]*Institute of Atmospheric Physics of Acad. Sci. Czech Rep., Boční II, 141 31 Prague 4, Czech Republic*
[2]*Space Research Institute, Russian Acad. Sci., Profsoyuznaya 84, 117810 Moscow, Russia*

ABSTRACT

Measurements onboard three Intercosmos satellites (IK 19, IK 24, and IK 25) yielded a data base of Te from periods of high solar activity. This data base has been used to construct global empirical model of Te in the region of 500 to3000 km altitude and ±90° invariant latitude. Individual submodels for two seasons (equinox, and solstice) and four different altitudes (550, 900, 1500, and 2500 km) were produced. They depend on invariant latitude and magnetic local time. Spherical harmonics up to the 8th order were used. Differences between our global model and IRI are analyzed.

INTRODUCTION

Thermal plasma parameters such as electron temperature (Te) and density (Ne) in the outer ionosphere have not yet been satisfactorily included in the most known ionospheric models such as the last version of IRI model (Bilitza 1990). Unlike electron temperature, electron density has been studied for a long time being the primary parameter needed for various applications connected mainly with electromagnetic wave propagation (Bilitza *et al.*, 1993). Therefore in this paper only the electron temperature model is described.

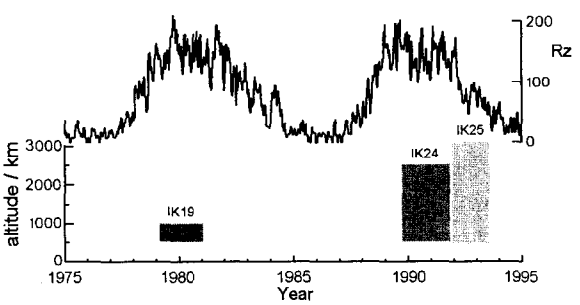

Fig. 1. Available data periods from Intercosmos 19, 24, and 25 satellites with corresponding solar activity, and altitude ranges.

Measurements by the Radiofrequency Probe and Retarding Potential Analyzer onboard the noncircularly orbiting Intercosmos satellites (IK 19, IK 24, and IK 25, see Table 1) yielded a data base of Te and Ne from periods of high solar activity (Figure 1). Partial models for low invariant latitudes (±30°) based on IK24 measurement only without analytical expression were shown in (Třísková *et al.*, 1996 and 1997). The whole data base has been used to construct a global analytical model of both parameters in the region of 500 to 3000 km altitude and ±90° invariant latitude. All model coefficients are available in computer form together with a program in IDL on request (e-mail: vtr@ufa.cas.cz) .

Table 1. Orbital parameters of IK 19, IK 24, and IK 25 satellites

satellite	perigee / km	apogee / km	inclination / deg	stabilization
Intercosmos 19	500	1000	74	three axis
Intercosmos 24	500	2500	83	three axis
Intercosmos 25	450	3100	83	three axis

The radio frequency method with three mutually perpendicular sensors (KM device) was used for the IK 24 and IK 25 satellites. Measured components: Tex along the velocity vector, Tey perpendicular to the orbit plane, and Tez towards the zenith, 10 sec averages were evaluated. For the model, minimum value (Temin) from Tex, Tey, and Tez was used to reduce the influence of hotter regions above the satellite and possible anisotropy of Te. For IK19 satellite only the Tex component was measured.

METHOD OF MODELING

All available Te data were grouped for seasons (80 day periods centered on equinoxes and solstices to ensure coverage at all local times by orbital precession) and for four altitude ranges: 550 ± 80 km, 900 ± 100 km, 1500 ± 250 km, and 2500 ± 500 km. Data from summer and winter hemispheres were coupled for solstices, for equinoxes data from both hemispheres were put together and symmetry was assumed.

Coordinate system

Magnetic local time (MLT) and invariant latitude (invl) were chosen as the principal coordinates. Invariant latitude for the Southern Hemisphere has been taken as negative. So, the influence of longitude on the Te pattern is reduced to a second order effect (Třísková *et al.*, 1997), and can be neglected in the first approximation. For modeling purposes it will be included together with other factors (solar activity and seasonal asymmetry) as perturbations on the global pattern where associated Legendre polynomials with a lower order will be used.

Analytical model

A system of associated Legendre polynomials up to the 8th order is employed for individual Te data groups. Thus expansion of Te was made in the following form:

$$Te = a_0^0 + \sum_{l=1}^{8} \left\{ a_l^0 P_l^0(\cos\theta) + \sum_{m=1}^{l} \left[a_l^m \cos m\varphi + b_l^m \sin m\varphi \right] P_l^m(\cos\theta) \right\} + R, \qquad (1)$$

where
P_l^m = associated Legendre function
φ = Invariant colatitude (0..π)
θ = Magnetic local time (0..2π)
R = residual part depending on second order factors

Associated Legendre polynomials P_l^m were used without normalization factors. These factors are included in coefficients a_l^m and b_l^m in Eq. (1) calculated by the standard method of a least squares fitting procedure. Before applying this fitting procedure, data (~10^5 points for each Te data group) were binned on a MLT vs. invl grid with variable bin number in dependence on data coverage. The minimum number of bins in the grid was 9 vs. 18 to guarantee coefficients fully recoverable and free of the alias effect (Martinec 1991). Te values

in each bin were separately averaged and corresponding standard deviations were evaluated for use in the fitting process as weights.

RESULTS

Contour plots of individual submodels representing global patterns of Te for corresponding altitudes and seasons are shown in Figures 2. through 5. It is apparent that mainly large scale features are represented. Temporal small scale structures such as the subauroral electron temperature enhancement are mostly washed out.

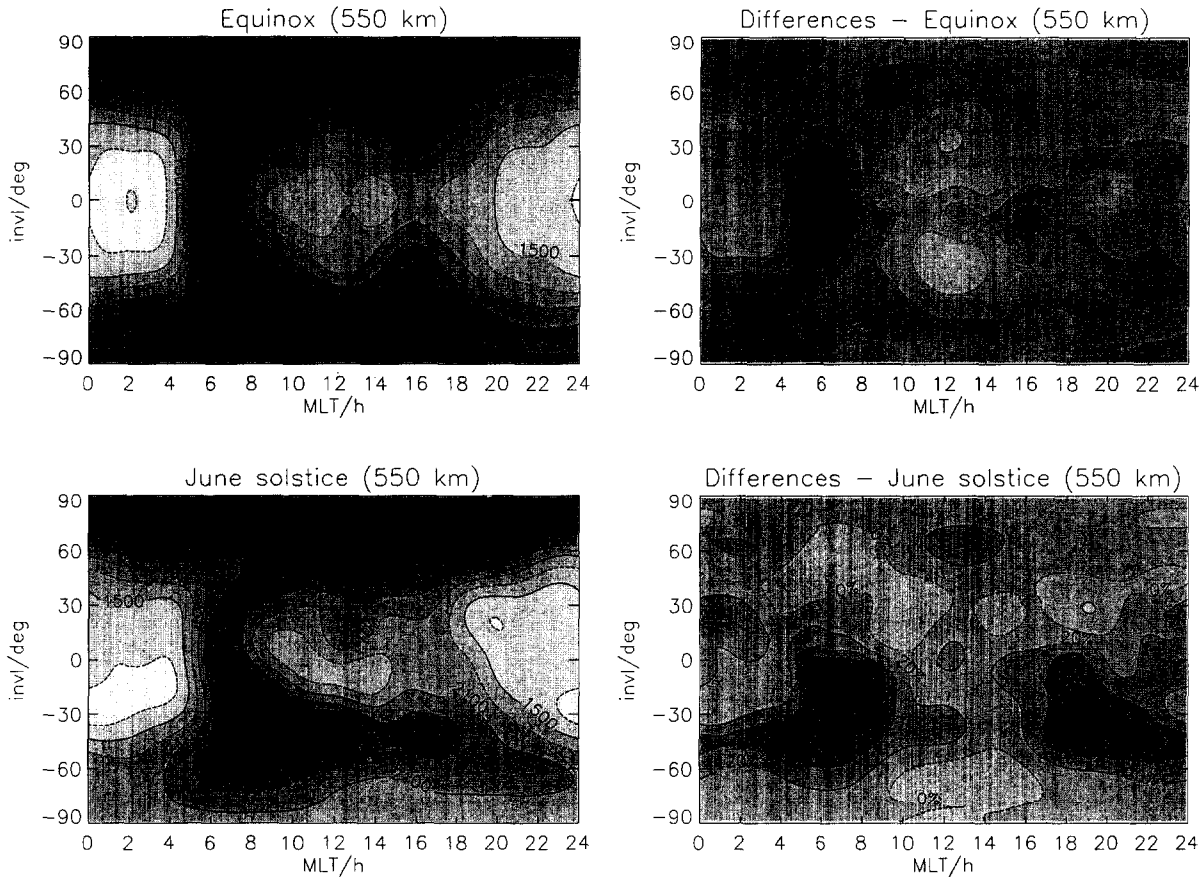

Fig. 2. Electron temperature distribution according to the proposed model in steps of 300K (left panels) and comparison with the IRI model, differences Δ in steps of 20% (right panels) for equinox and June solstice, $\overline{F10.7}$ = 185.

From the global model the following features of the Te distribution can be underlined:

- In general for a given MLT and invl, Te increases with altitude except in the polar caps for altitudes above 1500km where a zero or slightly negative gradient occurred (cf Yau *et al.*, 1995). At low latitudes (±30° invl) during the nighttime the Te altitude gradient is very small.
- Dependence of Te on MLT is characterized by the well known morning enhancement (morning overshoot) which is developed at equatorial latitudes and at low altitudes (550 to 900 km). For solstices its maximum is shifted to the the winter hemisphere (cf Oyama *et al.*, 1996).
- Dependence on invariant latitude is more prominent at lower altitudes (550 to 1000 km). Generally the lowest electron temperature is observed close to the equator and increases with increasing invariant latitude.

At solstices during the day the winter hemisphere Te is slightly higher than the summer one in low and lower middle latitudes. Illuminated polar regions are hotter then the shadowed ones.

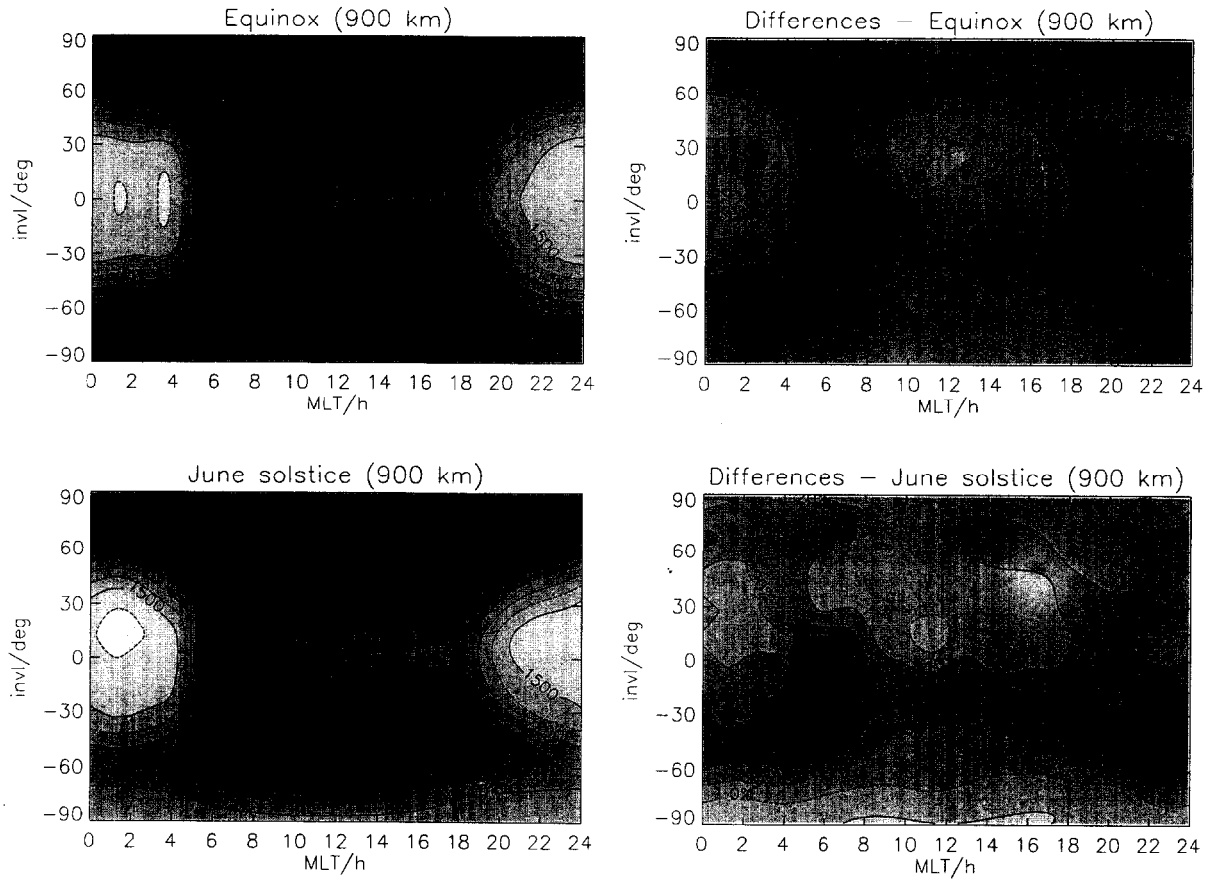

Fig. 3. Electron temperature distribution according to the proposed model in steps of 300K (left panels) and comparison with the IRI model, differences Δ in steps of 20% (right panels) for equinox and June solstice, $\overline{F10.7}$ ~ 185.

Comparison with IRI model

For comparison of the presented model with IRI the Te distribution in the invl vs MLT was calculated for corresponding altitudes and seasons. Differences between both models were evaluated as follows:

$$\Delta = \frac{Te_{model} - Te_{IRI95}}{Te_{IRI95}} \times 100\% \qquad (2)$$

This comparison allows to formulate following statements:

- IRI does not include the morning overshoot at altitudes 550 and 900 km. In the model by Brace and Theis (1981) which represents the principal part of the IRI Te model, the morning overshoot in the level of 400 km is well expressed but at altitude above ~500 km this phenomenon is washed out in IRI due to the included model by Spenner and Plugge (1979) which does not cover sunrise hours.

- In general IRI temperatures are lower by 0 to 40% at 550 and 900 km during both solstice and equinox. At the altitude of 1500 km the difference is typically 0 to 20% with exception of the winter hemisphere where differences are up to -20%. The best agreement of both models is at the 2500 km altitude where differences are typically -20 to 0%. Additionally there are limited regions of greater differences before sunrise and after sunset.

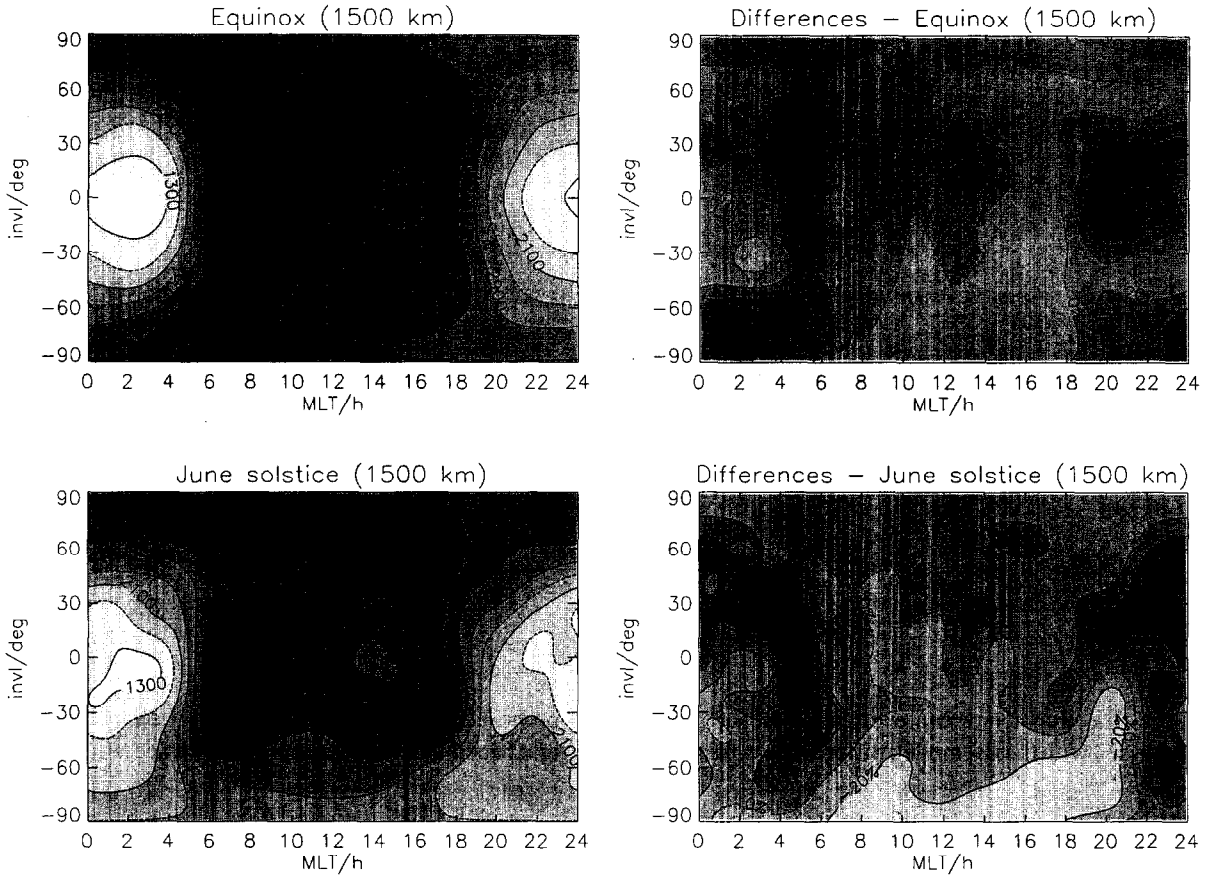

Fig. 4. Electron temperature distribution according to the proposed model in steps of 300K (left panels) and comparison with the IRI model, differences Δ in steps of 20% (right panels) for equinox and June solstice, $\overline{F10.7}$ ~ 185.

CONCLUSION

Global model of Te for high solar activity based on approximation by spherical harmonics at four different altitudes is presented. Individual submodels describing behavior of Te in dependence on the first order parameters are shown. Further improvement including other influences namely the solar activity is intended. Comparison with IRI shows in general differences of less than +20%, extremes being -20 to 100%, responding to the physical processes in specific parts of the MLT vs. invl vs. altitude space.

ACKNOWLEDGMENT

This research was partially supported by grants No. A3042603/1996 and No. A3042703/1997 of the Grant Agency of Academy of Sciences of the Czech Republic.

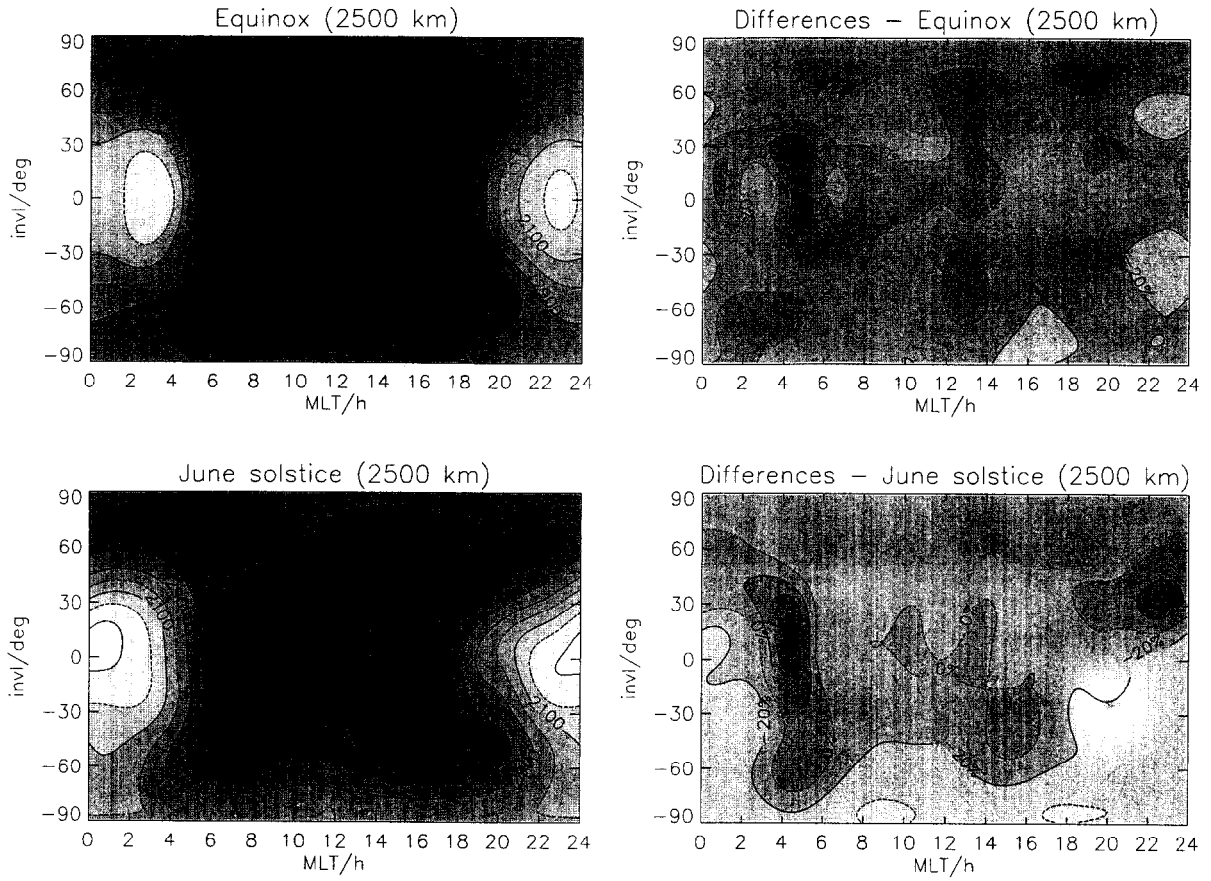

Fig. 5. Electron temperature distribution according to the proposed model in steps of 300K (left panels) and comparison with the IRI model, differences Δ in steps of 20% (right panels) for equinox and June solstice, $\overline{F10.7}$ ~ 185.

REFERENCES

Bilitza D.,International Reference Ionosphere 1990, National Space Science Data Center, NSSDC 90-22, Greenbelt, Maryland (1990).

Bilitza D., K. Rawer, L. Bossy, and T. Gulyaeva, International Reference Ionosphere - Past, Present, and Future: II. Plasma Temperatures, Ion Composition and Ion Drift, *Adv. Space Res.*, **13**, (3)15 - (3)23 (1993).

Brace L.H., and R. F. Theis, Global empirical models of ionospheric electron temperature in the upper F-region and plasmasphere based on in situ measurements from Atmosphere explorer C, ISIS 1 and ISIS 2 satellites, *J. Atmos. Terr. Phys.*, **43**, 1317-1343(1981).

Martinec Z., Program to calculate the least-squares estimates of the spherical harmonic expansion coefficients of an equally angular-gridded scalar field, *Comp. Phys. Communications*, **64**, 140-148(1991).

Oyama K.-I., W. Watanabe, Y. Su, T. Takahashi, and K. Hirao, Season, Local Time, and Longitude Variations of Electron Temperature at the Height of ~600 km in the Low Latitude Region, *Adv. Space. Res.*, **18**, (6)269 - (6)278 (1996).

Spenner K., and R. Plugge, Empirical model of global electron temperature distribution between 300 and 700 km based on data from AEROS-A, *J. Geophys.*, **46**, 43-56(1979).

Třísková L., J. Šmilauer, V. Truhlík, and V. V. Afonin, On the Low Latitude Topside Models: II. Electron Temperature, *Adv. Space Res.*, **18**, (6)213 - (6)216 (1996).

Třísková L., J. Šmilauer, V. Truhlík, and V. V. Afonin, Contribution to Modelling the Electron Density and Temperature in the Disturbed Low Latitude Topside Ionosphere, *Adv. Space Res.*, **20**, (9)1741 - (9)1744 (1997).

Yau, A. W., B. A. Whalen, T. Abe, T. Mukai, K. I. Oyama, and T. Chang, Akebono Observations of Electron Temperature Anisotropy in the Polar wind, *J. Geophys. Res.*, **100**, 451-463 (1995).